J. Fluid Mech. (1983), *vol.* 137, *pp.* 233–250
Printed in Great Britain

The control of boundary-layer transition using a wave-superposition principle

By ANDREW S. W. THOMAS
Lockheed-Georgia Company, Marietta, Georgia, U.S.A.

(Received 28 January 1983)

An experimental study has been made of the concept of controlling boundary-layer transition by superimposing in the flow Tollmien–Schlichting waves that are of equal amplitude and antiphased to the disturbances that grow and lead to transition. The cases that have been considered are transition arising from a single-frequency two-dimensional disturbance and transition arising from a nonlinear interaction between two waves of different frequency. A feedback system for controlling transition has also been studied. In each case, both hot-wire surveys and flow visualization have shown that it is possible to delay transition but that the flow cannot be restored completely to its undisturbed state. This appears to be a consequence of interactions between the very weak three-dimensional background disturbances in the flow and the primary two-dimensional waves. The implications of these findings in an implementation of the concept are discussed.

1. Introduction

Because transition in a boundary layer arises from the growth of instability waves in a flow, a possible method of controlling and delaying transition is by the use of wave superposition, or what has sometimes and perhaps incorrectly been called wave cancellation. The principles are straightforward enough and merely require the introduction into the flow of a disturbance of necessary phase and amplitude so as to cancel any existing instabilities through superposition. That this might be possible is a consequence of the linear nature of the Orr–Sommerfeld equation that describes these instabilities.

The first reported evaluation of the concept was in a brief study performed by Milling (1981) in a water channel. He used a vibrating wire to introduce instabilities into the flow and another wire a short distance downstream to introduce the control disturbances. The separation of his wave generators corresponded to about four Tollmien–Schlichting wavelengths, and he reported moving transition to beyond the end of his test plate or, in dimensionless terms, from a Reynolds number of 520000 to one in excess of 670000. Unfortunately, no data were presented describing the level of background disturbances in the flow or the spectral evolution of the controlled flow.

In a study carried out at the same time in a water tunnel at Caltech, Liepmann, Brown & Nosenchuck (1982) used heating strips to excite instability waves in a laminar boundary layer. Similar heating strips were located downstream in order to excite the control disturbances. Downstream attenuation of the instability waves and a delay in transition were evident. This wave-generation technique is easier in water than in air because of the very good thermal coupling that can be achieved with water and the strong temperature dependency of its viscosity. In an extension of this study, Liepmann & Nosenchuck (1982) used a hot-film sensor to measure the fluctuations

existing in the boundary layer, and from this they synthesized a signal to drive the cancellation disturbance. This gave them an active feedback control of transition. They did not report any detailed measurements of the flow that remained after the cancellation procedure.

Thus, although control of boundary-layer transition using a wave-superposition principle has been demonstrated in different facilities, a number of questions arise. Not the least of these is the question of what is left in the flow after this procedure is used and whether or not it is possible to use this technique to return a flow to its completely undisturbed state.

Furthermore, experiments have shown that, when transition arises from the breakdown of two-dimensional instability waves, strong three-dimensional distortions of the wavefronts can be observed, leading to an array of vortex loops or 'lambda'-shaped vortices. Because this gives rise to adjacent maxima and minima in the spanwise distribution of disturbance amplitude, this is sometimes referred to as the peak–valley structure of transition. In the past the occurrence of this three-dimensionality has incorrectly been attributed to the use of vibrating ribbons to excite the flow, but this cannot be the case since it has also been observed under conditions when no ribbons are present (Knapp & Roache 1968).

It has now become apparent that the development of the three-dimensionality during boundary-layer transition, even if excited at a single frequency, arises from interactions between the primary wave and other disturbance waves in the flow. These disturbances have their origins with the freestream, and the primary wave provides an environment in which they can amplify more than would be possible from linear physics. The triad mechanism described by Craik (1971) is an example of such a resonance mechanism. Thomas & Saric (1981) have also demonstrated that the character of the interactions that take place can differ according to test conditions and that two different modes of transition can arise when ostensibly the same amplitude of primary disturbance is used to excite the flow. This can have serious implications in a transitional control scheme where control is applied mainly to the primary disturbance in the flow. The question that then arises is whether or not any realistic control can be exercised over the wave interactions as well or whether all the control must be exercised before any of these nonlinear interactions take place.

The present series of experiments were undertaken in order to clarify some of these issues.

2. Experimental considerations

The experiments that will be described were undertaken in a low-turbulence wind tunnel that has a 0.6 m × 0.9 m test section that is 6.5 m in length. This facility is identical with the tunnels used by a number of universities actively involved in boundary-layer research and provides a freestream turbulence level that is of the order of 0.03–0.05 % of the freestream velocity. The upper and lower walls of the test section are flexible for pressure-gradient control and were set to give constant pressure over the flat test plate used in the present series of tests.

The flat plate itself is shown in figure 1. It was made of a highly polished aluminium honeycomb panel and had a 0.9 m span and a 2.3 m chord. It was mounted in the vertical plane of the wind-tunnel test section and a 0.3 m chord flap was used at the trailing edge to control the leading-edge stagnation point. This gave rise to a small region of favourable pressure gradient at the leading edge, but zero pressure gradient was maintained over the last 2 m of the plate. The favourable-gradient region

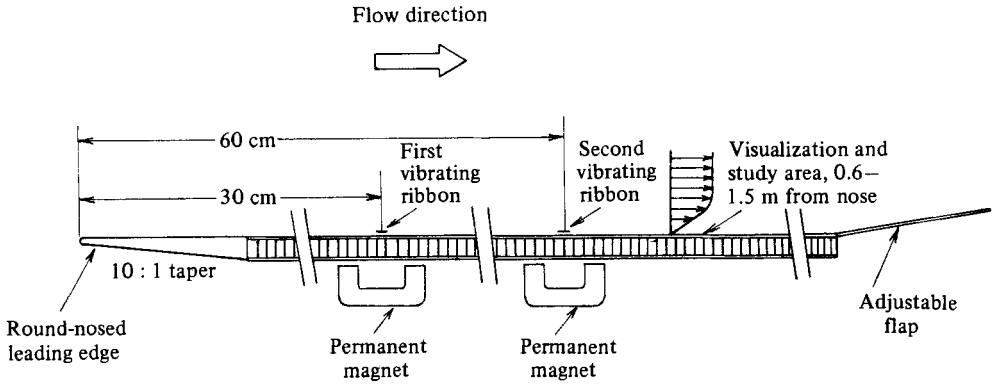

FIGURE 1. The flat-plate configuration used in the present series of studies.

manifests itself downstream as a slight change in the effective origin from which the Blasius boundary layer develops. Subsequent measurements have shown this to be small, and it has therefore been ignored in the presentation of the experimental results.

Electromagnetically excited vibrating ribbons (2.5 mm wide and 0.05 mm thick) were used to generate the instability waves in the flow, and, as depicted in figure 1, these were located 0.3 and 0.6 m from the leading edge. Small plastic shims of 0.4 mm thickness were used to space the ribbons from the plate, and only the central 0.6 m of the ribbons were allowed to oscillate. Permanent magnets below the plate provided the magnetic field to the ribbons, and power amplifiers were used to drive the excitation current through the ribbons. Variable-relative-phase sinusoidal signals were generated by a Hewlett-Packard 203A variable-phase function generator.

The smoke-wire technique was used to visualize the developing flowfields, and for this purpose a 0.075 mm (0.003 in.) diameter stainless-steel wire was stretched across the plate at a distance of 0.45 m from the leading edge and at a height of 1.2 mm from the plate surface. This height corresponds approximately to the critical layer of the instabilities in the flow. Light machine oil was allowed to drip down the wire to moisten it, and the wire was then electrically heated for approximately 1 s to create the filaments of smoke. A spring was used to apply preload to the wire to prevent bowing or vibrations when heated with the d.c. current.

The effect of the presence of this wire on the flow was examined in some detail and was found to be non-negligible. The findings of this study are discussed in the Appendix, from which it is concluded that useful data can be obtained provided that the wire is present throughout the entire test program. Thus, to ensure consistent test conditions between the hot-wire data and the visualization tests, even when not in use, the smoke wire was left in its operational position on the plate.

The hot wires used in this test program were driven in the constant-temperature mode and were 5 μm unetched and unplated tungsten wires of 1.2 mm length. For the surveys of the mean flow and of the disturbance flow they were mounted on a three-axis traverse system that was driven by stepper motors coupled to the wind-tunnel minicomputer to provide a positional accuracy of 0.015 mm.

The same minicomputer was also used to drive the data-acquisition system, so that, coupled with the traverse system, it was an easy matter to obtain the growth of the total disturbance down the test plate.

Spectral data were also recorded at selected locations during this test program and these were obtained using a Nicolet 660A dual-channel FFT analyser.

3. Mean-flow parameters

For most of the data to be reported, the mean freestream velocity was 8.5 m/s, although one visualization study taken at 5.4 m/s will also be reported. Surveys of the unexcited mean flow were made at various streamwise locations to ensure that the developing boundary layer behaved as a Blasius-type flow.

The flow quality over the plate was such that 'natural' transition (that is, transition arising from the amplification of the background disturbances) did not take place before the trailing edge of the plate. At this speed, this location corresponds to a Reynolds number of one million and by running the tunnel at higher speeds it has been found that the natural transition Reynolds number for this facility is in excess of 5×10^6. This is close to the highest value reported by Spangler & Wells (1968) in a study of the effects of freestream disturbances on transition, and serves as some measure of the good quality of the flow within the facility.

In terms of the mean-flow parameters that were measured, the non-dimensional locations of the two ribbons as well as the region of study are shown in figure 2 relative to the neutral-stability curve for two-dimensional Tollmien–Schlichting waves. For this and subsequent figures the streamwise coordinate is represented by the square root of the streamwise Reynolds number since this is the relevant parameter for Blasius boundary-layer flow.

The primary instability frequencies that were used in this study were nominally 80 and 100 Hz, which correspond to dimensionless frequencies of $F = 110$ and 137 respectively, where $F = 10^6 \times 2\pi f\nu/U_0^2$. These are also depicted in figure 2, from which it can be seen that the study region extends from within the neutral-stability curve to beyond branch II. Also shown in figure 2 are lines depicting the corresponding regions of study of Liepmann *et al.* (1982) and Milling (1981). The small vertical bars on these lines correspond to the locations of their wave-generator pairs. It is evident that, in dimensionless terms, the present wave generator pair are further apart than in the other studies. This point will be returned to later.

4. Control of transition arising from single-frequency waves

The first experiment used a single-frequency signal to excite instability waves from the first ribbon at a frequency of 80 Hz or $F = 110$. The amplitude of the disturbance was adjusted to cause transition to take place at about the middle of the study region. The growth of the total disturbance in the boundary layer has been measured and is shown in figure 3. (In this and subsequent figures, the data were recorded at a position corresponding to the maximum in the distribution of the disturbance amplitude across the layer.)

It can be seen that the wave initially grows according to a linear theory, but, when an amplitude of about 2% of the freestream velocity is reached, a period of much more rapid growth takes place and transition can be said to have occurred.

A frequency-locked disturbance of variable relative phase was then applied to the second ribbon, and both its phase and amplitude were iteratively adjusted to minimize the disturbances measured at a point 140 cm downstream of the leading edge of the plate. A tracking filter of 10 Hz bandwidth was used to aid in identifying the amplitude of the 80 Hz component at this location. Figure 3 shows the measured disturbance growth of the resulting wave in isolation as well as the measured growth obtained when both wave generators are in use. It is gratifying to see that the required control disturbance is initially of the same amplitude as that of the wave which arises

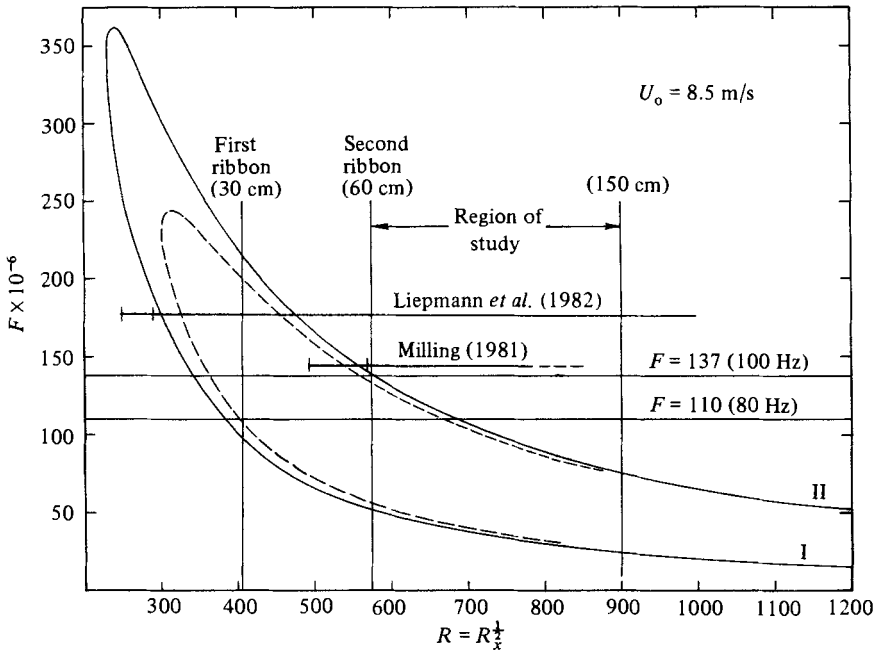

FIGURE 2. The locations of the vibrating ribbons and the region of study relative to the neutral-stability diagram. The dashed curve corresponds to the limits based on a parallel stability analysis. Also shown are the experimental conditions of Liepmann *et al.* (1982) and Milling (1981).

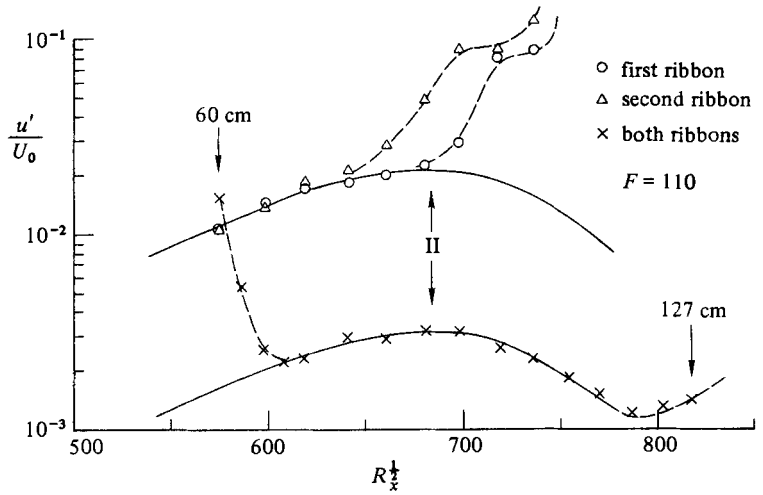

FIGURE 3. The streamwise growth of an instability wave of frequency $F = 110$ (80 Hz) arising from the first ribbon, the second ribbon and both ribbons when the optimal phase- and amplitude-control conditions exist.

from the first ribbon. However, this is not and should not be expected to be the case when transition begins, because the different upstream wave histories lead to different possible forms of wave interaction that may take place.

When the two waves are superimposed, the total disturbance amplitude in the layer initially increases, but it is very quickly reduced by about an order of magnitude within one or two wavelengths of the second ribbon. The disturbance that remains

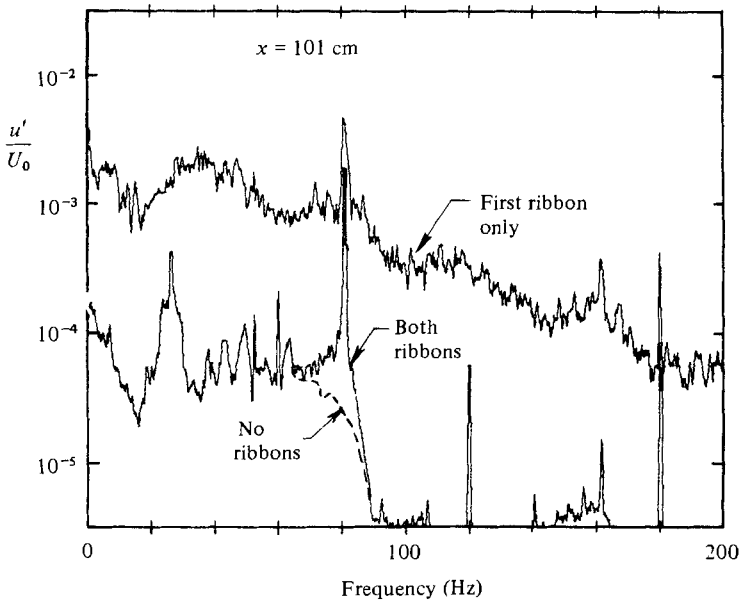

FIGURE 4. The spectrum of the velocity fluctuations in the boundary layer for a wave of frequency $F = 110$ arising from the first ribbon. Also shown is the spectrum obtained for the optimal control conditions in figure 3.

is of much lower amplitude and then grows and behaves as expected from linear theory. However, a point is reached further downstream where it too begins to depart from linear theory.

The spectra of the fluctuations corresponding to this test condition are shown in figure 4 at a location corresponding to $R_x^{\frac{1}{2}} = 730$. When only the first ribbon is used, it can be seen that the spectrum of the velocity fluctuations has a broadband character with a readily identifiable peak at 80 Hz. A broadband peak centred around 40 Hz can also be identified along with a similar peak at 120 Hz. Evidently, for this particular case transition is taking place by a subharmonic wave interaction as described by Thomas & Saric (1981).

Spectral levels are dramatically reduced when the second ribbon is in operation, and the spectrum is very similar to that which is obtained if no excitation is present on either ribbon. An exception can be seen at and around 80 Hz, where some energy still remains that would otherwise not be present. (The peaks at 60, 120 and 180 Hz correspond to electronic noise of the anemometer system and can be ignored.)

These data therefore show that delays of transition have been achieved, but that it has not been possible to return the flow completely to its base state with the superposition scheme.

Smoke-wire visualizations have been undertaken to demonstrate this further, and these are shown in figures 5 and 6. The flow visualization shown in figure 5 is the base flow obtained with no excitation present on either ribbon. The smoke filaments are smooth and reasonably straight and the flow is quite obviously laminar. Some small perturbations can be seen in the smokelines and these arise from the background disturbances in the flow and are of low level. It must be remembered when examining pictures such as these that they depict streaklines and contain the effect of a long integrated history. Thus, even quite a large perturbation on a smokeline does not imply a large-amplitude disturbance. It can also arise from a very-low-amplitude disturbance that has had sufficient time to act and distort the smokelines.

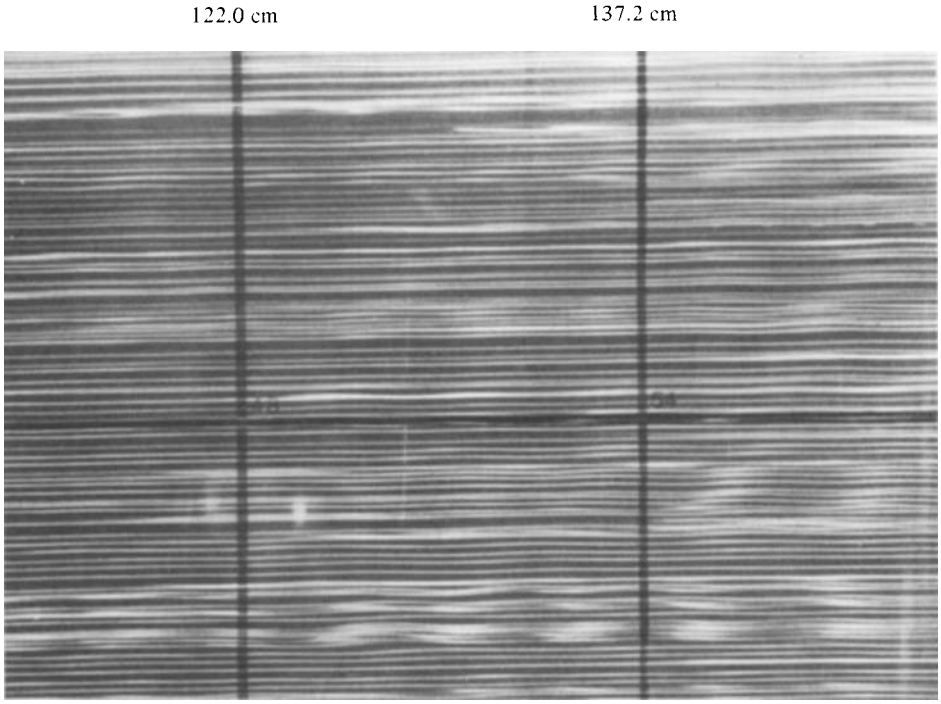

FIGURE 5. A smoke-wire visualization of the undisturbed boundary-layer flow. In this and subsequent visualizations the flow is from left to right and the gridlines on the plate are at 15.25 cm (6 in.) spacing.

When excitation is applied to the first ribbon alone, the visualization shown in figure 6(*a*) is obtained. It can be seen that the waves in the boundary layer soon develop three-dimensionalities and distortions in the spanwise direction. An array of 'lambda' vortices then forms, with the peaks of the lambdas on adjacent waves displaced laterally from one another. This is the staggered peak–valley structure described by Thomas & Saric (1981) and is the kind of structure that would be expected from the observed occurrence in the spectrum of a subharmonic component at 40 Hz. When the control disturbance is present the visualization shown in figure 6(*b*) is obtained. This shows the flow in a region somewhat further downstream than in figure 6(*a*) and it can be seen that the flow is indeed laminar to a higher Reynolds number. However, it can also be seen that there are three-dimensional distortions on the wavefronts which ultimately give rise to transition.

Comparison with figure 5 suggests that it has not been possible to return the flow to its undisturbed base state. However, it must also be noted that visual observation of the presence of wavefronts in the controlled flow does not by itself necessarily imply the presence of real disturbances in the flow. This is because of the memory of the streakline effect discussed previously and the fact that the smoke wire was located before the second ribbon. Thus the smoke streaklines have an opportunity to distort before the primary disturbance is removed and this distortion will remain after the control disturbance is introduced. Indeed, on this basis one should expect to see apparent wavefronts even if the disturbances were completely removed. However, the fact that three-dimensional distortions can be seen on the smoke filaments in an otherwise two-dimensional experiment is good evidence for the presence of three-dimensionalities that were not present in the base flow.

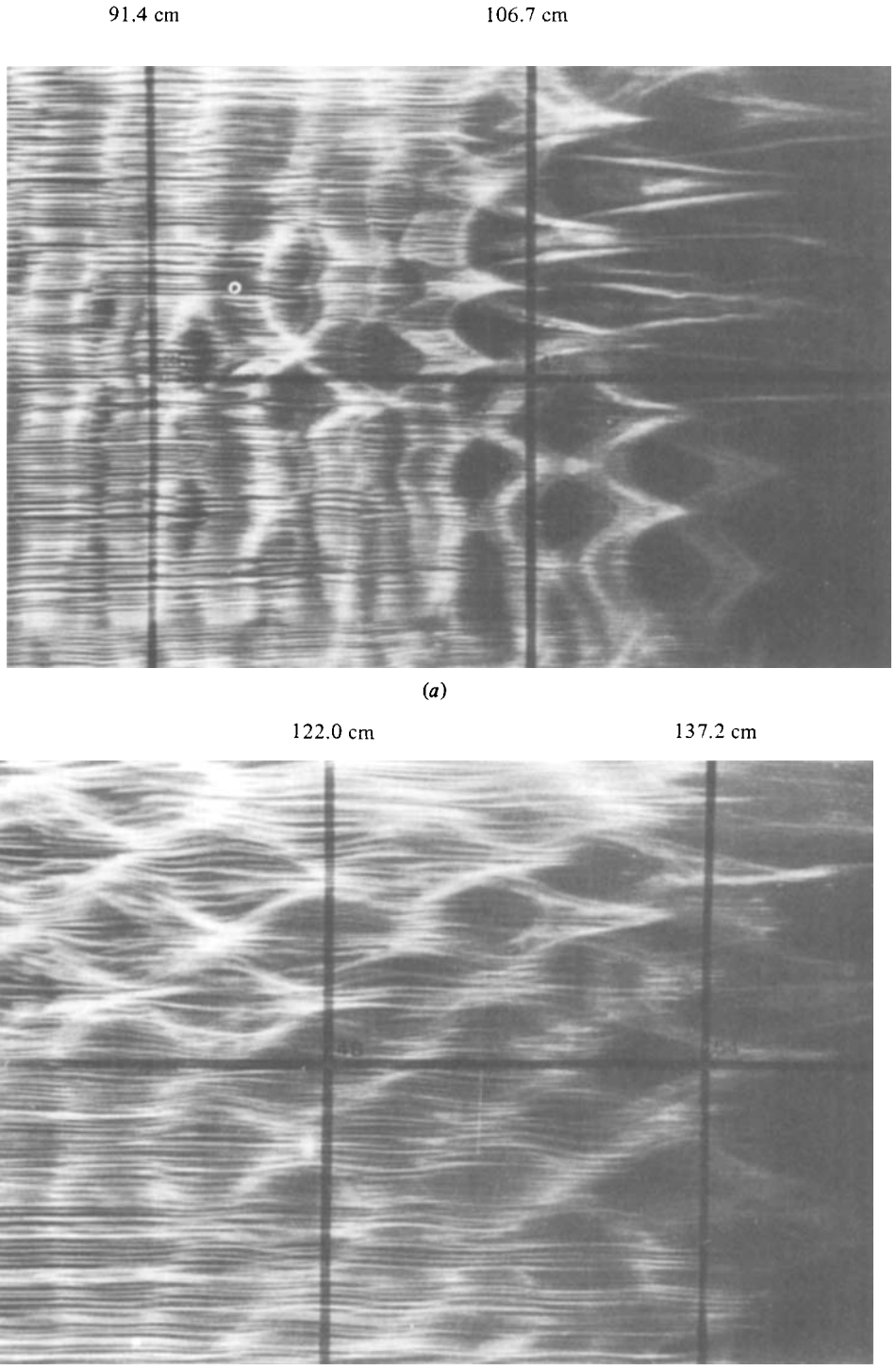

FIGURE 6. Smoke-wire visualization of the flow conditions corresponding to those of figure 3: (*a*) excitation from the first ribbon alone; (*b*) excitation from both ribbons. Note that (*b*) is taken further downstream than (*a*).

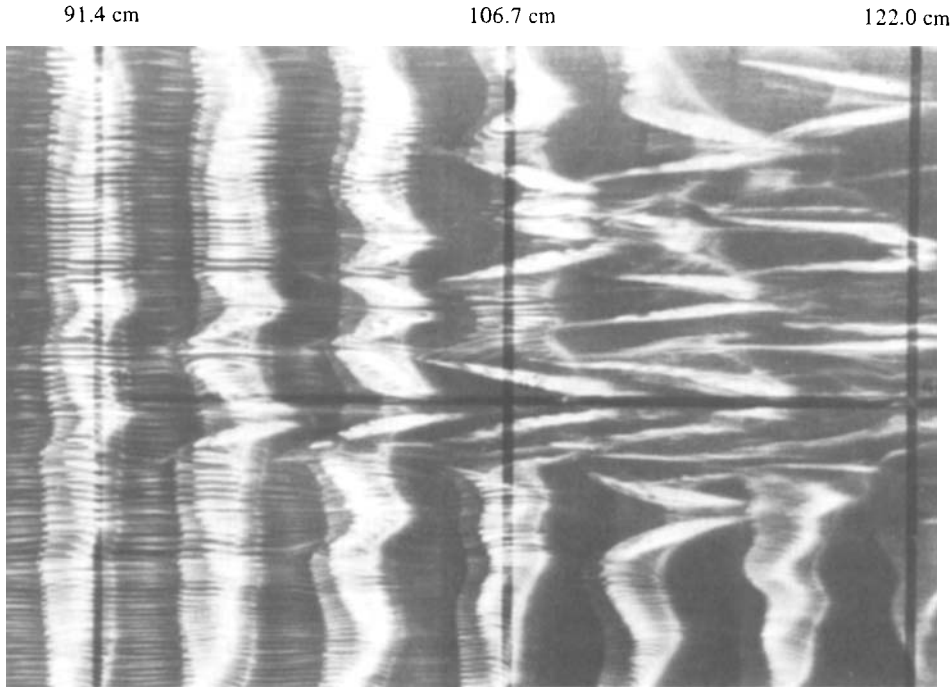

(*a*)

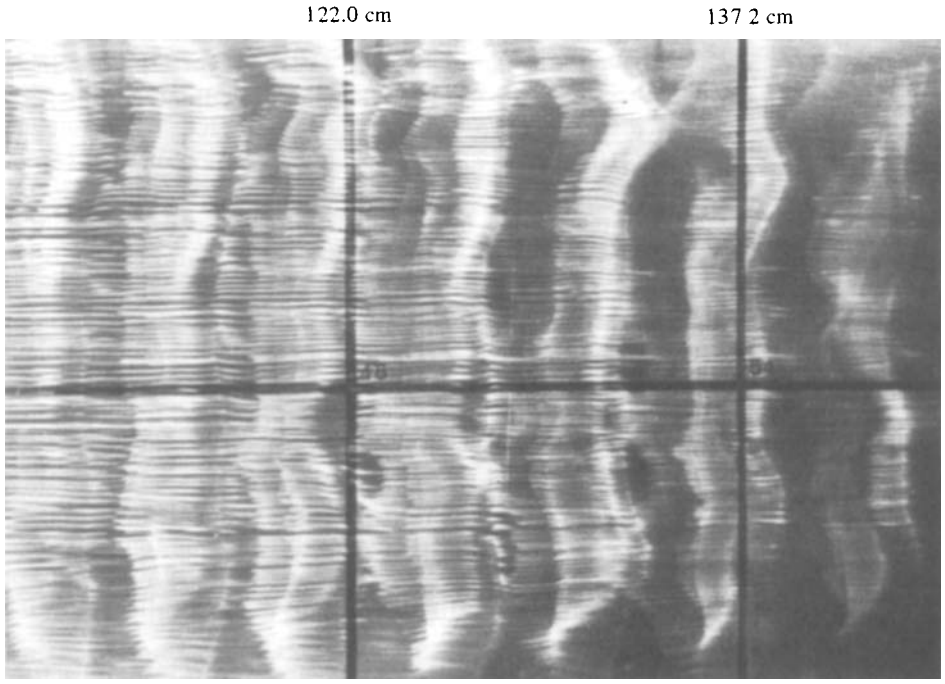

(*b*)

FIGURE 7. Smoke-wire visualization of the control of a wave of frequency $F = 127$ (37 Hz) at a freestream velocity of 5.4 m/s: (*a*) excitation from the first ribbon alone; (*b*) excitation from both ribbons when optimal control conditions of phase and amplitude are present.

The same experiment has also been repeated at a lower tunnel speed, and the corresponding visualizations are shown in figures 7(*a*, *b*). It can be seen in this case that, when excitation arises from the first ribbon alone, the mode of transition is now one in which the developing vortex loops are all aligned as in the ordered peak–valley structure reported by Thomas & Saric (1981). When the control disturbance is applied, transition has been significantly delayed, although once again distortions can be seen on the residual wave. The flow has not returned to its undisturbed base state. (The distortions being referred to can be seen on the wavefronts in the centre of the picture. Other disturbances can be seen at the top and bottom of the picture, but these arise from contamination from the ribbon supports and should be ignored.)

5. Control of transition arising from wave interactions

A likely explanation of the observed behaviour is that three-dimensional disturbances that arise from the freestream are amplified through an interaction with the environment of the primary instability disturbance that is created at the first ribbon. Craik (1971) has described a possible mechanism by which this can happen. Although the primary disturbance is then removed or reduced at the second ribbon, the three-dimensional disturbances still remain and have an amplitude that is greater than that which would have arisen if the primary instability had not been present. If this is the case, then it suggests that interactions between waves are preventing the flow from being driven back to its base state.

The question of wave interactions has been examined in greater detail by undertaking a two-dimensional experiment in which the first ribbon was driven by a waveform consisting of the sum of two sinusoids of 80 and 100 Hz ($F = 110$ and 137 respectively). The amplitude of each frequency component was adjusted to give the spectral development depicted in figures 8(*a*, *b*). It is evident that, in this case, transition did not arise directly from the 80 or 100 Hz components, but from a strong interaction at the difference frequency of 20 Hz. Kachanov, Koslov & Levchenko (1980) and Saric & Reynolds (1980) have also reported observing such an interaction. Figures 9(*a*–*c*) depict the streamwise growth of each frequency component. The 80 and 100 Hz components display linear behaviour before the transition region, but a rapid increase in the amplitude of the 20 Hz component is evident and this is taking place in a region where linear stability theory predicts decay. This is due to a nonlinear interaction between the two primary oscillations.

Also shown in the figures are the wave growths that are obtained when the amplitude and phase of the 80 and 100 Hz signals on the second ribbon are adjusted to minimize the downstream disturbances. It can be seen that the wave amplitudes required to do this are comparable to those arising from the first ribbon. It can also be seen that, when both ribbons are in operation, then reductions in the amplitudes of the 80 and 100 Hz frequency components are observed. Also, although the amplitude of the 20 Hz component is initially increased, it begins to decay also. At $R_x^{\frac{1}{2}} \approx 750$, however, it begins to amplify once again, and the point at which this happens corresponds closely to the branch I curve of the neutral-stability diagram for that frequency.

Visualizations of this flowfield were performed and are shown in figures 10(*a*, *b*). Figure 10(*a*) corresponds to the case when excitation is on the first ribbon alone and shows the character of transition when it takes place through the difference-frequency interaction. In the right-hand part of the photograph a region of developing peaks and valleys can be seen. Further upstream and $\frac{1}{20}$ s behind them, another smaller

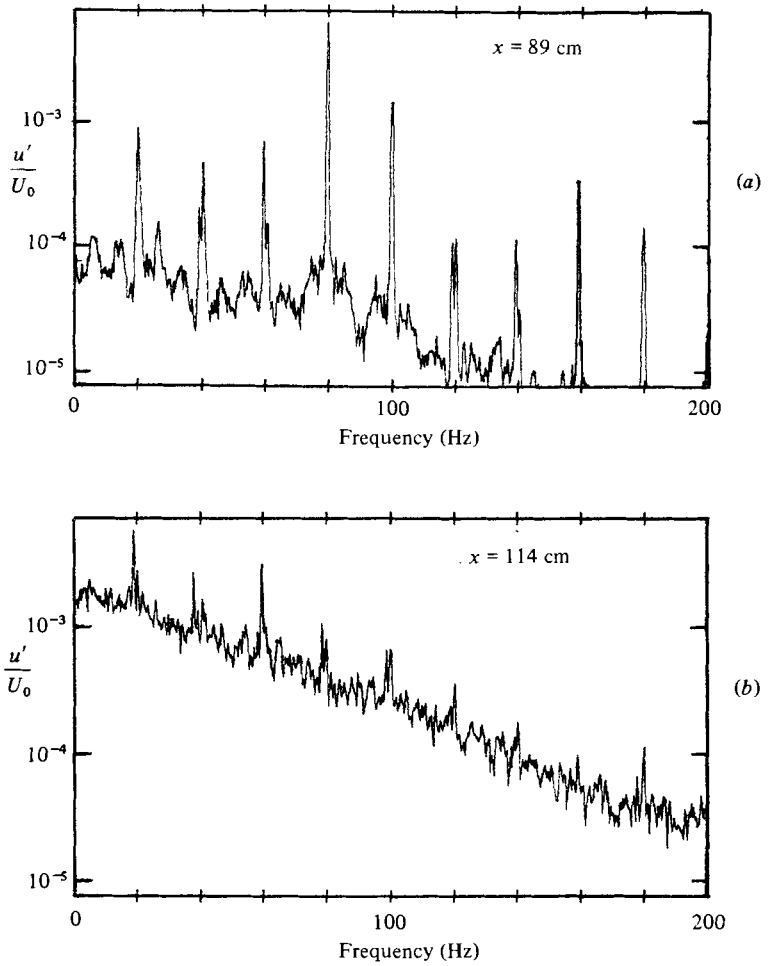

FIGURE 8. The spectral development of the disturbances when excitation of two frequencies of 80 and 100 Hz (F = 110, 137) is applied to the first ribbon: (*a*) x = 89 cm; (*b*) x = 114 cm.

region of developing peaks and valleys can be seen starting to form. It is noted that the existence of the low-frequency 20 Hz component does not lead to an increase in the scale of the observed transitional lambda-vortex structure but causes these structures to occur in modulated groups.

When the optimal cancellation condition is established, the visualization in figure 10(*b*) is obtained. The flow is certainly much smoother, but low-amplitude three-dimensionalities can again be observed. These are residual disturbances in the flow that are not present in the undisturbed base flow shown in figure 5.

It is clear from these data that if the control disturbance is introduced at a point where the primary oscillations are still linear, but where nonlinearities have begun to occur through interaction with other frequencies, full control will not be achieved. The use of a third ribbon further down the plate and driven at the difference frequency might have removed some of the energy of the residual 20 Hz disturbance. However, as shown by figure 10(*b*) there are three-dimensional disturbances associated with this component and no two-dimensional control could be exercised over these residual waves.

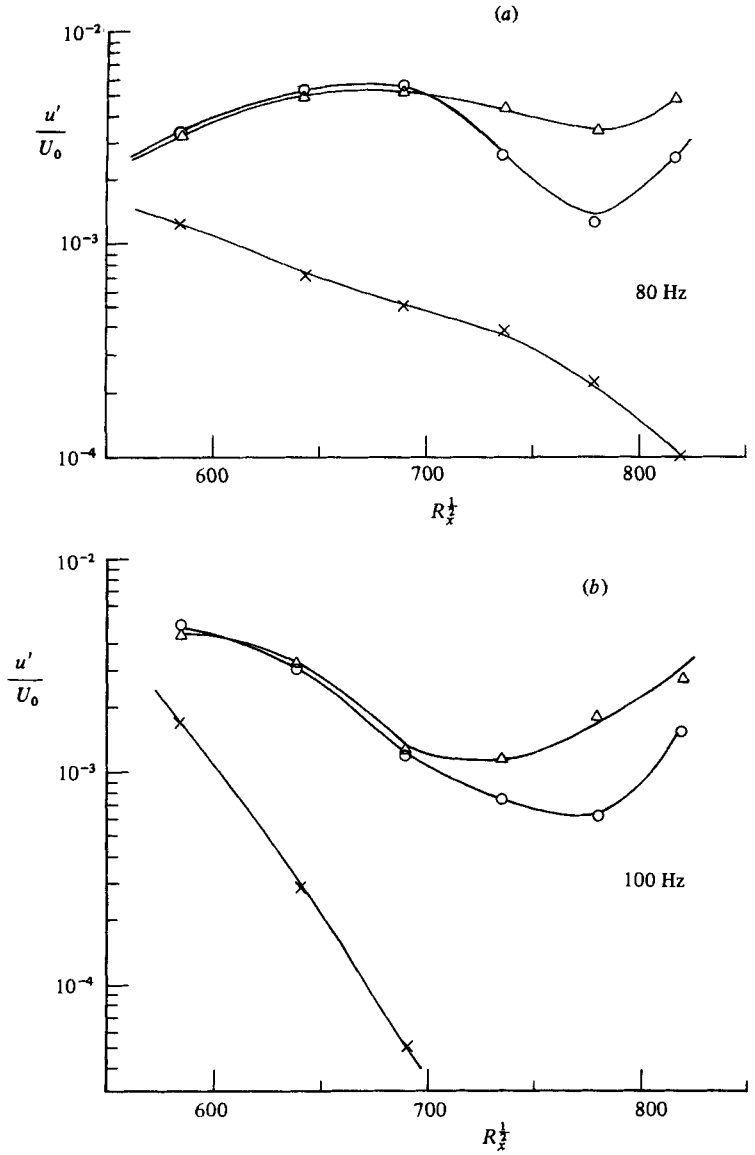

FIGURE 9(*a*, *b*). For caption see facing page.

6. Feedback control of transition

The present experiments have been concerned with waves that are excited by constant-amplitude signals. In any real implementation of this method to control transition, the incoming waves would have varying amplitude so that some real-time detection of local wave amplitude would be needed. In fact one can envisage a drag-reduction scheme in which a sensor in the flow detects the frequency and phase of all the pretransitional disturbances. A control circuit would then be used to synthesize an appropriate phase- and amplitude-corrected signal to cancel the disturbances further downstream and delay transition. Liepmann & Nosenchuck (1982) used such a system to delay transition in a water tunnel. However, their configuration was greatly simplified by the fact that the background disturbances in

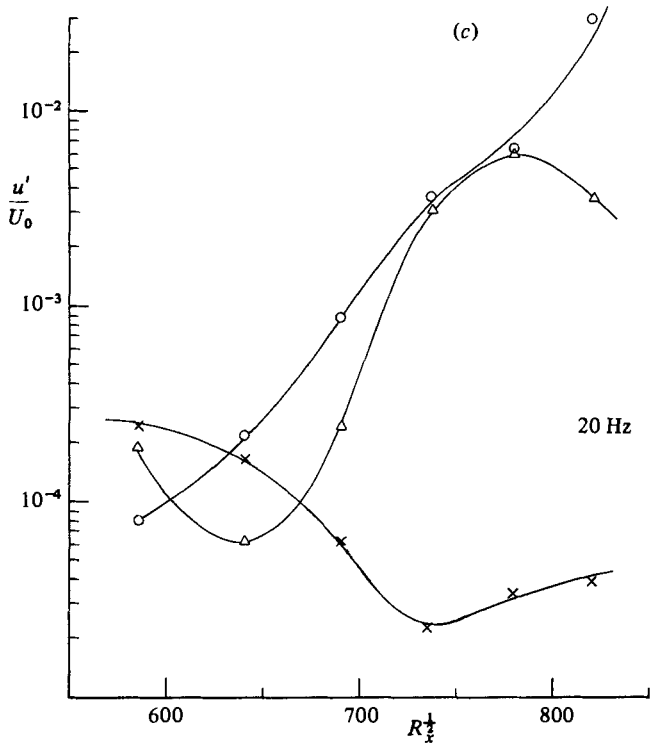

FIGURE 9. The streamwise growth of the (*a*) 80 Hz, (*b*) 100 Hz and (*c*) 20 Hz waves when excitation is applied to the first ribbon alone (○), the second ribbon alone (△) and both ribbons with optimal settings of phase and amplitude at 80 and 100 Hz (×).

the flow were nearly constant-amplitude sinusoids to begin with, so that a phase shift was essentially all that was needed to obtain the cancellation wave.

The same control system was also set up during the present test program, and a miniature hot wire was embedded in the plate one half-wavelength ahead of the second ribbon to detect the boundary-layer fluctuations. An instability wave was excited from the first ribbon and the output of the hot wire was used to create a driving signal for the second ribbon. Because of the half-wavelength spacing, this yielded a disturbance that was locally 180° out of phase with the wave from the first ribbon. These tests were performed at 80 Hz and yielded the same kind of results as depicted in figure 3 previously. It was particularly gratifying to see that, as the amplitude of the first wave was varied by adjusting the oscillator output, then, after an appropriate delay, smooth flow was automatically obtained downstream once again.

The delay in this system arose partly from the need to maintain a half-wavelength spacing to obtain correct phase. Such a system would not be suitable for random disturbances and, to attempt to overcome this, the wire was positioned, instead, immediately above the second ribbon. Excitation of the first ribbon using sinusoids and band-limited white noise was studied and the inverted output of the hot wire was used to synthesize the control signal. However, in each case local disturbances from the flow around the ribbon distorted the output of the hot wire so that its signal was unusable for control.

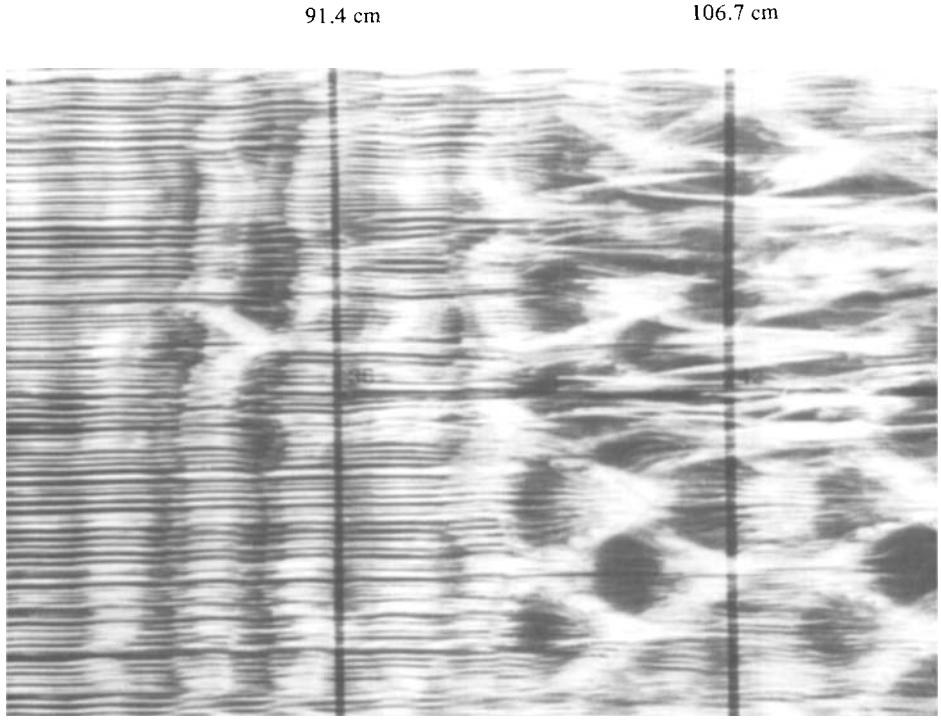

(*a*)

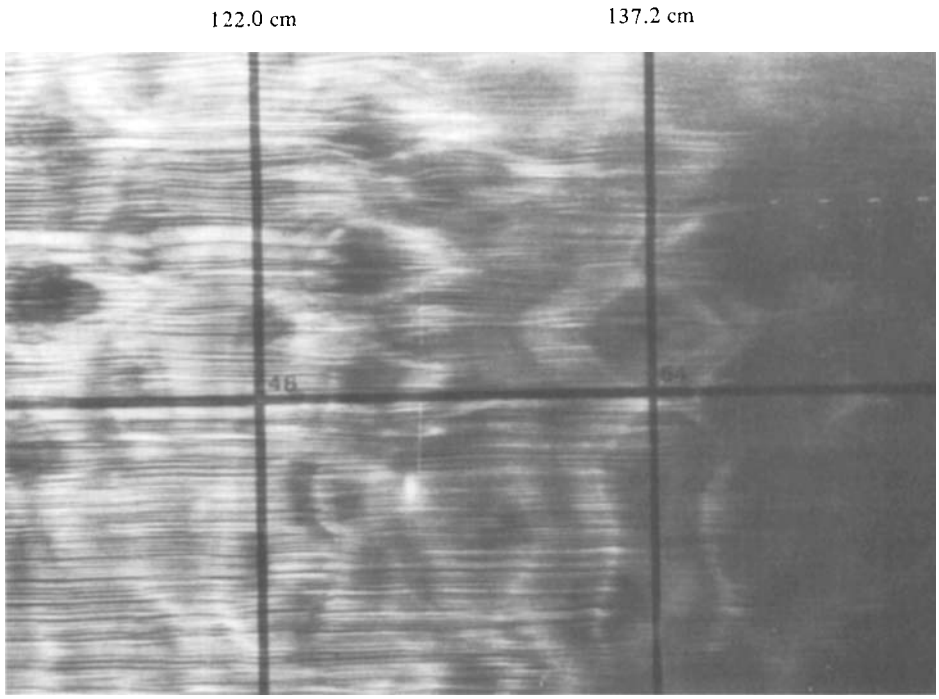

(*b*)

FIGURE 10. Smoke-wire visualization of the flow conditions corresponding to figure 9: (*a*) excitation from the first ribbon alone; (*b*) excitation from both ribbons with optimal amplitude and phase settings.

7. Discussion and summary

It has been demonstrated through hot-wire and flow-visualization methods that it is possible to delay transition by a wave-superposition scheme. This has been achieved for the case of single-frequency waves by superposition of an equal-amplitude and antiphased disturbance. This leads to a downstream reduction in the amplitude of the primary disturbance and delay in transition from a Reynolds number of 490000 to about 810000. However, interaction between the primary disturbance and background disturbances led to an increase in the level of background three-dimensional disturbances so that it was not possible to completely return the flow to its undisturbed state.

To examine the consequences of wave interactions further, the same control method has been used to control transition arising from the interaction of two waves of different frequency. In that case the primary waves were behaving linearly but a nonlinear interaction gave rise to a low-amplitude difference frequency that ultimately led to transition. Using the control method, the amplitudes of both of the primary disturbances could be reduced. However, the amplitude of the difference-frequency component could only be partially reduced, and this wave in turn interacted with background three-dimensional disturbances in the flow. Because of the three-dimensionalities and the nonlinearity, further two-dimensional control of the residual disturbances would probably not have been successful.

Thus, in both this and in the previous case, because of wave interactions, it has not been possible to eliminate transition and return the flow completely to its undisturbed base state. For this reason, it is probably more appropriate to describe this transition control method as wave superposition rather than wave cancellation.

To implement the concept it will be important to minimize the effect of the interaction. This can be done by minimizing the duration of the time that the flow is exposed to the interaction, that is by minimizing the residence time of the waves. In other words, it is important to inject the control disturbance as soon as possible after the primary disturbance. Referring back to figure 2, it can be seen that the tests of Liepmann *et al.* (1982) and Milling (1981) used a smaller dimensionless spacing between the input and cancellation generators than in the present study so that no strong wave interaction would have had time to develop in those cases.

The problem that then arises in a real application of this control concept is that the initial disturbances will enter the boundary layer not at a discrete point as in the present tests, but over a region or some receptive area around and near the leading edge. Thus there may always be some residence time associated with any wave, even if it is removed as soon as it has become detectable. Wave interactions are therefore likely, particularly since they can arise at quite low amplitudes when the primary disturbances are still behaving linearly. For example, in the present tests even waves of amplitudes less than 1 % gave rise to interactions. A realistic control system should therefore probably need to take account of possible complex wave interactions in addition to the control of the primary linear disturbances.

Furthermore, even if the effect of these interactions can be minimized, some residual disturbances are likely to remain after the control method is employed and other new disturbances may enter the boundary layer downstream. Successive and more complex control systems can be conceived, but, on a real application at higher Reynolds numbers, the growth of these waves would eventually become explosively large and the thresholds to initiate transition would become smaller and smaller. These effects will work in opposition to one another so that, while the ultimate control of transition in such cases is conceptually feasible, its implementation will be difficult.

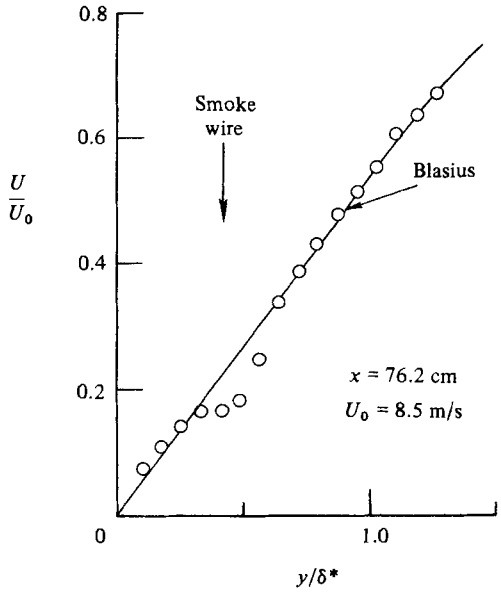

FIGURE 11. The mean-velocity profiles in the region just downstream of a smoke wire that is 1.2 mm from the surface and 76.1 cm from the leading edge.

The author is particularly grateful to Dr W. S. Saric of Virginia Polytechnic Institute and State University for useful discussions during the course of this work. The experiments were supported by the Independent Research and Development program of the Advanced Research Organization of the Lockheed-Georgia Company.

Appendix. The use of a smoke wire in boundary-layer transition studies

Although the findings of the present work have, where possible, been substantiated by hot-wire surveys, much use has also been made of flow visualization using the smoke-wire method. It is therefore worthwhile examining the effect that this wire has on the flow.

In order to satisfactorily visualize instability waves it is necessary that the wire, whose diameter in the present tests was 0.075 mm, be positioned near the critical layer of the instabilities. In these low-speed tests this is usually about 1.2 mm from the surface. At this position it will leave a wake in the flow. A mean-velocity profile recorded just downstream of a moistened wire is shown in figure 11, from which it can be seen that a small near-wall velocity defect can be observed. Surveys taken further downstream show that this disappears about 5 cm downstream of the wire. The wake is laminar and the wire does not trip the flow at the low speed of the tests.

In transition studies the main consequence of this wake is that, because it modifies the mean profile, it also modifies the stability characteristics of the flow. This is demonstrated by the wave-amplitude data shown in figure 12. When the wire is removed, different amplitude-growth curves are all parallel when plotted on a logarithmic amplitude scale. This is because the waves are growing and behaving according to linear theory. When the wire is present it leads to an increase in linear wave growth downstream of the wire. This effect persists for about 10 cm and then the wave behaviour is once again the same as it was when the wire was not present. In one case that is presented, the wire increased the wave amplitude sufficiently to bring about transition but this is merely a consequence of the large amplitude. It

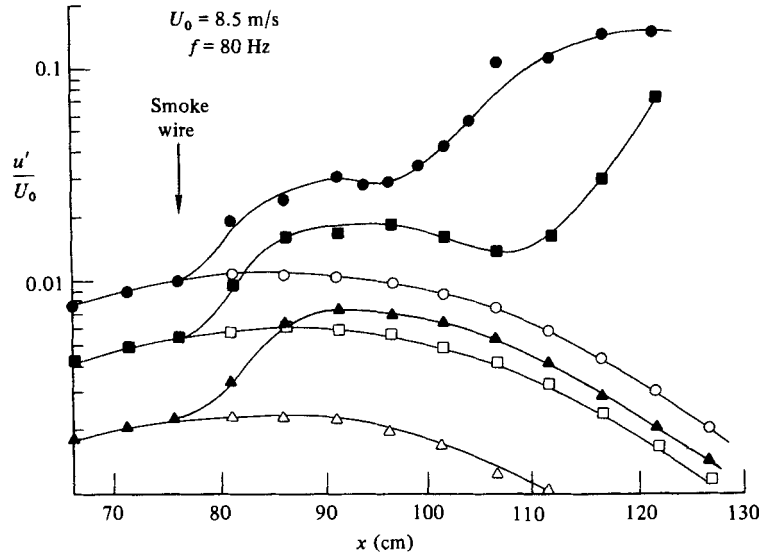

FIGURE 12. The growth of instability waves of frequency 80 Hz and various amplitudes as they pass over the smoke wire (solid symbols) and when the smoke wire is not present (open symbols).

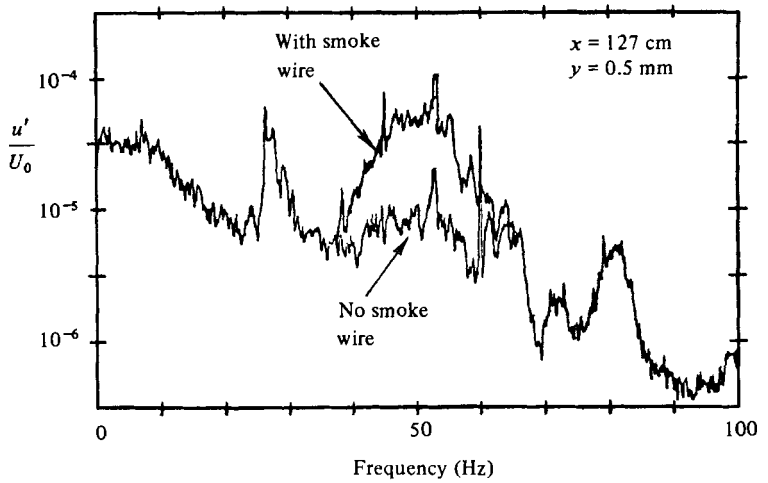

FIGURE 13. The spectrum of the background velocity fluctuations in the boundary layer when the smoke wire is present and when it is absent. The smoke wire is located at x = 76.1 cm.

is not a consequence of something spurious originating from the wire. Therefore, other than changing the amplitude at which the ribbon must be operated, the effect of the wire on an instability wave can be tolerated.

The only shortcoming of this is that it will also affect the amount of amplification that background disturbances will undergo. For example, figure 13 shows the spectrum of the velocity fluctuations that are obtained 0.5 mm from the plate, at x = 127 cm when no ribbon excitation is present. These therefore represent the background disturbances in the flow, and it can be seen that the presence of the wire has led to increases in certain frequency bands. Since the wire diameter is such that its shedding frequency would be very high and that, in any case, its Reynolds number is too low for shedding to occur, even when wet, this increased level must result from

slight amplification of the background disturbances. To maintain constant flow conditions it is therefore important to undertake all tests with the wire in place and moistened with oil. This was the case in the present series of tests and a visualization of the base flow has been shown in figure 5 previously.

Finally, spectral data were obtained with a constant heating voltage applied to the wire to examine the effect of any thermal influences. The spectrum that was obtained is exactly the same as the cold-wire case shown in figure 13 showing that thermal effects are not important.

REFERENCES

Craik, A. D. D. 1971 *J. Fluid Mech.* **50**, 393.

Kachanov, Tu. S., Koslov, V. V. & Levchenko, V. Ya. 1980 In *Laminar–Turbulent Transition* (ed. R. Eppler & H. Fasel). Springer.

Knapp, C. F. & Roache, P. J. 1968 *AIAA J.* **6**, 26.

Liepmann, H. W., Brown, G. L. & Nosenchuck, D. M. 1982 *J. Fluid Mech.* **118**, 187.

Liepmann, H. W. & Nosenchuck, D. M. 1982 *J. Fluid Mech.* **118**, 201.

Milling, R. W. 1981 *Phys. Fluids* **24**, 979.

Saric, W. S. & Reynolds, G. A. 1980 In *Laminar–Turbulent Transition* (ed. R. Eppler & H. Fasel). Springer.

Spangler, J. G. & Wells, C. S. 1968 *AIAA J.* **6**, 543.

Thomas, A. S. W. & Saric, W. S. 1981 *Bull. Am. Phys. Soc.* **26**, 1252.